

A Frequency Domain Approach for Controlling Fast-Scale Instabilities in Switching Power Converters

E. Rodriguez, E. Alarcón
Electronic Department, UPC-BarcelonaTech
Barcelona, 08034, Spain
enric.rodriguez@upc.edu, eduard.alarcon@upc.edu

H. H. C. Iu
Department of Electronic, Electrical Engineering
University of Western Australia, Perth, 6009, Australia
herbert@ee.uwa.edu.au

A. El Aroudi
Departament d'Enginyeria Electrònica, Elèctrica i Automàtica
Universitat Rovira i Virgili, Tarragona, 43007, Spain
abdelali.elaroudi@urv.cat

This paper deals with controllers of fast-scale instabilities in DC-DC switching power converters from a frequency domain standpoint with the aim of understanding their working principle and hence simplifying their design. Some approaches for controlling fast-scale instabilities and their limitations are revisited. Considering the frequency domain transfer function of already existing controllers, a simple and extended notch filter centered at half of the switching frequency is proposed to avoid these instabilities. However, a switching converter under this controller may still exhibit the undesired slow-scale instability. Accordingly, the paper explores an alternative approach based on amplifying the harmonic at the switching frequency. Numerical simulations show that the new proposed controller can concurrently improve both fast-scale and slow-scale stability margins. The results from the different controllers are contrasted in terms of stability boundaries, indicating that the last one presents a wider stability range.

1. Introduction

Switching power converters are used in many power management applications due to their potential for high efficiency and size reduction, despite they tendency to exhibit instabilities [Krein & Bass, 1990; Fossas & Olivar, 1996; Mazumder *et al.*, 2001; Chen *et al.*, 2008; Xiong *et al.*, 2013; Zhao *et al.*, 2013]. Keeping high efficiency whilst guaranteeing stability is becoming challenging, especially for the new trends in power management which demands further miniaturization and even on-chip integration of switching power converters [Allard *et al.*, 2004]. This requires to reduce the reactive components size, leading to an increase of switching frequency in order to keep the same dynamics, which is in turn limited due to efficiency constraints. This limitation results in an increase of converter output voltage ripple rendering the system to be more prone to exhibit the so-called fast-scale instabilities (FSI) [Rodriguez *et al.*, 2012]. This work considers a voltage-mode controlled (VMC) buck converter with a PI compensator with transfer function $G_c(s) = k_p(s + \omega_{z1})s^{-1}$ along with an additional circuitry, namely an additional controller $G_{FS}(s)$ to avoid

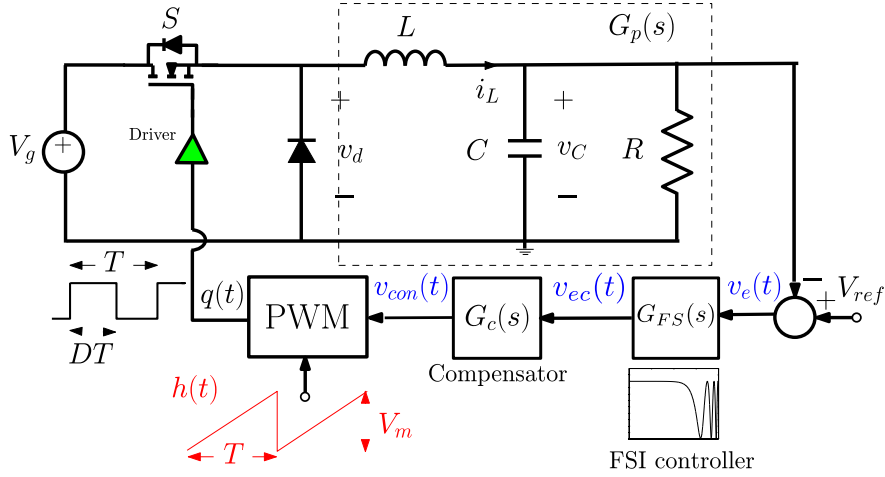


Fig. 1. VMC buck converter with a compensator $G_c(s)$ along with a FSI controller $G_{FS}(s)$.

the exhibition of FSI, as it is shown in Fig. 1. The exhibition of these kinds of instabilities is shown in Fig. 2 by increasing the proportional gain. A period-doubling bifurcation scenario is clearly observed giving rise to sub-harmonic oscillations and ending up in chaotic behavior. FSI instabilities are characterized by the exhibition of sub-harmonics at multiple of the switching frequency until the behavior turns into a chaotic regime. Switching power converters can also exhibit other instabilities such as slow-scale instabilities (SSI), characterized by a low-frequency oscillation.

Figure 2 was obtained by sweeping the controller gain and plotting a steady state representative state variable (capacitor voltage) sampled at the switching frequency rate. Increasing the proportional gain has been chosen as a simple way of increasing the ripple amount in the control path without modifying the loop phase, but other approach to increase the ripple, such as reducing the inductance value or the switching frequency, will also lead to occurrence of such instabilities [Rodriguez *et al.*, 2012]. The following nominal parameters used are used aiming the miniaturization of the converter: $V_g = 6$ V, $V_{ref} = 3$ V, $f_s = 50$ MHz, $V_m = 1$ V, $L = 66$ nH, $C = 20$ nF, $R = 2.5$ Ω and $\omega_{z1} = 1$ Mrad/s.

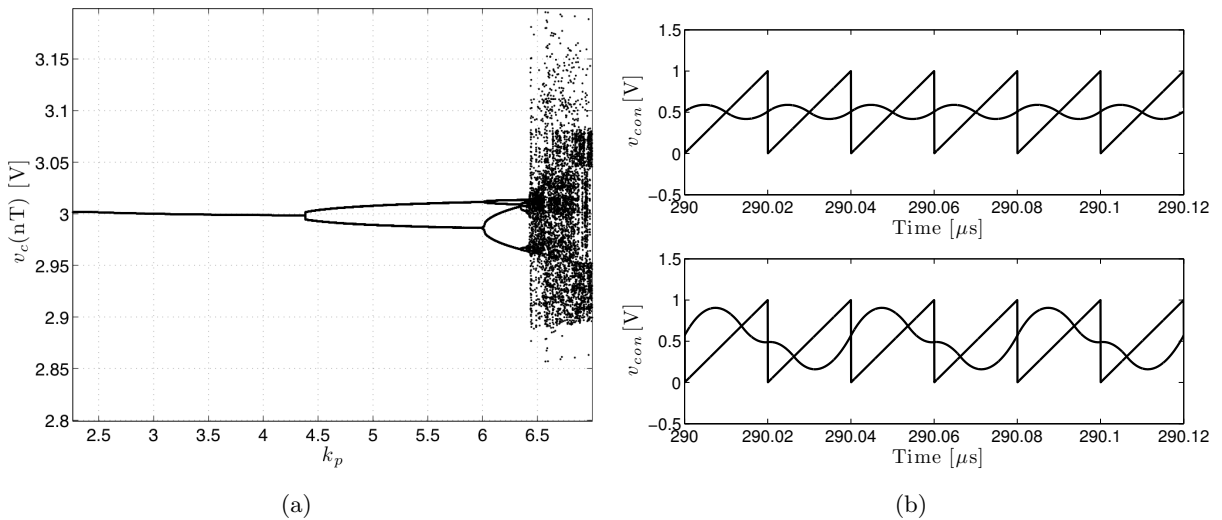


Fig. 2. (a) Bifurcation diagram by increasing k_p showing the route to chaos via period-doubling. $k_{p,crit} = 4.3$. (b) Time-domain modulator input waveform v_{con} showing period-1 behaviour when $k_p = 3$ (top plot) and period-2 behaviour when $k_p = 5$ (bottom plot).

In the past, in less demanding applications, the dynamics modeling of such converters has hitherto been

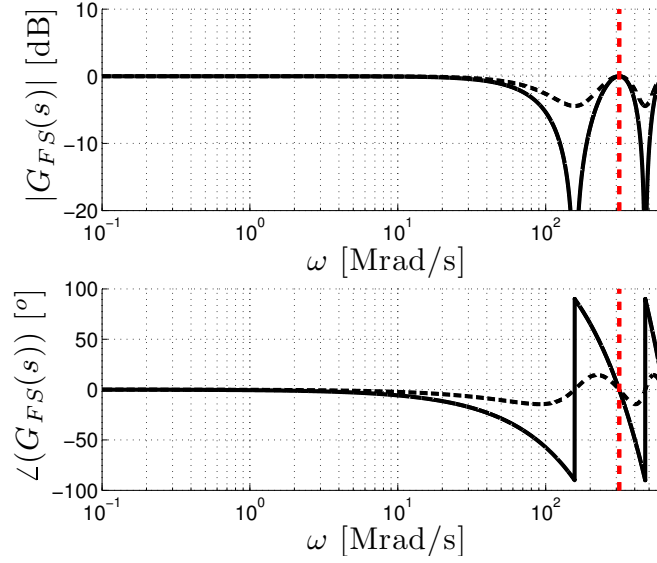


Fig. 4. Bode diagram representation (magnitude and phase) of the TDFC with $\gamma=0.2$ and (dashed) $\gamma=0.5$ (solid). Vertical dashed line indicates the switching frequency.

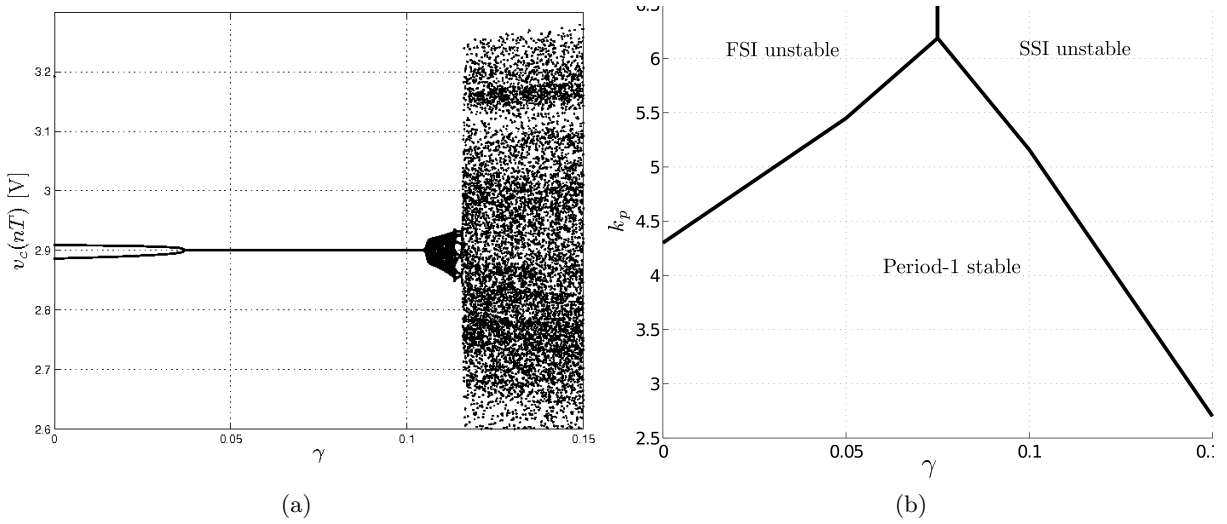


Fig. 5. (a) Bifurcation diagram by sweeping γ in a VMC buck converter with TDFC for proportional gain $k_p=5$ (in period-two without TDFC). (b) Stability boundary between Period-1, FSI and SSI as a function of γ and k_p . $k_{p,crit}=4.3$ (without controller)

2.1. The time-delay feedback controller

This section explores the frequency response of the TDFC, obtained from particularizing the transfer function given in Eq. (1) for $\beta=0$.

The frequency-domain representation depicted in Fig. 4 for different values of the parameter γ , shows that the controller provides a frequency-selective comb-filter which attenuates the harmonics at half of the switching frequency and its integer multiples. Note that the controller has a *non-invasive* nature since it does not modify neither the DC component, nor the harmonic at the switching frequency. As it can be observed, by increasing γ , the attenuation increases (only for γ up to 0.5), and an additional phase lag is added.

The effect of γ upon exhibition of FSI is shown in Fig. 5. This figure shows that the controller leads to improve the FSI boundary (even avoiding the chaotic behaviour), but with some strong limitations

within the design-space. Namely, on the one hand, there exists a critical minimum value of γ to avoid FSI exhibition, which depends upon the amount of ripple in the converter, considering the direct relationship between fast-scale stability and ripple demonstrated in [Rodriguez *et al.*, 2012]. On the other hand, simulation results show that for a certain critical value of γ (which does not depend upon the ripple) the TDFC yields to exhibit SSI. This is in agreement with the phase response given in Fig. 4 for which higher values of γ lead to adding a phase lag to the loop gain, hence making the converter prone to exhibit SSI. This fact, detrimental to SSI, opposes to the controller benefits in terms of FSI hence compromising the overall stability of the system.

2.2. Extended time-delay feedback controller

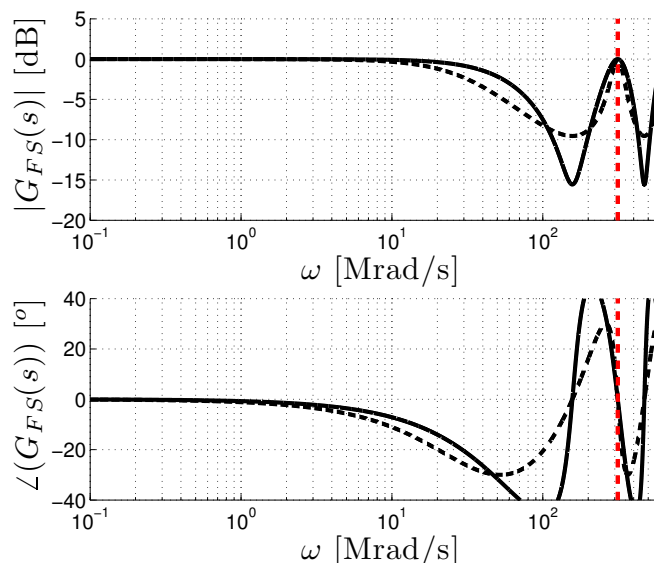


Fig. 6. Bode diagram representation (magnitude and phase) of the ETDFC with $\gamma=0.5$ and $\beta=0.2$ (solid) and $\beta=0.5$ (dash). Vertical dashed line indicates the switching frequency.

The ETFDC includes an additional feedback inner loop depending upon a new parameter β as it is shown in Fig. 3. Fig. 6 shows the effect of such parameter upon its frequency response. By increasing the value of β and keeping γ constant, the phase response is smoothed, but on the other hand the attenuation at half of the switching frequency decreases. In fact, this trade-off allows to use higher values of γ than in the TDFC case, as it is shown in Fig. 7-a, hence improving the FSI boundary, but requiring a higher minimum value of γ to control the instability.

Fig. 7-b shows the stability boundary surface, obtained from numerical simulations, by sweeping both γ and β parameters. For low values of β and high values of γ , SSI is exhibited, whereas, as β is increased, the system is more prone to exhibit FSI.

Regardless of the stability improvement in the ETDFC, both time-delay-based controllers have some important limitation in terms of design and implementability. The first one arises because of the trade-off between SSI and FSI exhibition, which requires a proper selection of γ and β parameters to avoid these instabilities. The lack of a clear criteria to set up these parameters values leads to require a proper exploration as it has been carried out in this section. The second one arises from the implementation difficulties of time-delay-based controllers since both of them are based on a delay module whose implementation is challenging in the analog domain.

3. Notch-filter-based chaos controllers

The chaos controllers studied in the previous section are based on eliminating the sub-harmonic components from the feedback path to avoid the exhibition of FSI, by means of a delay-based structure, which has

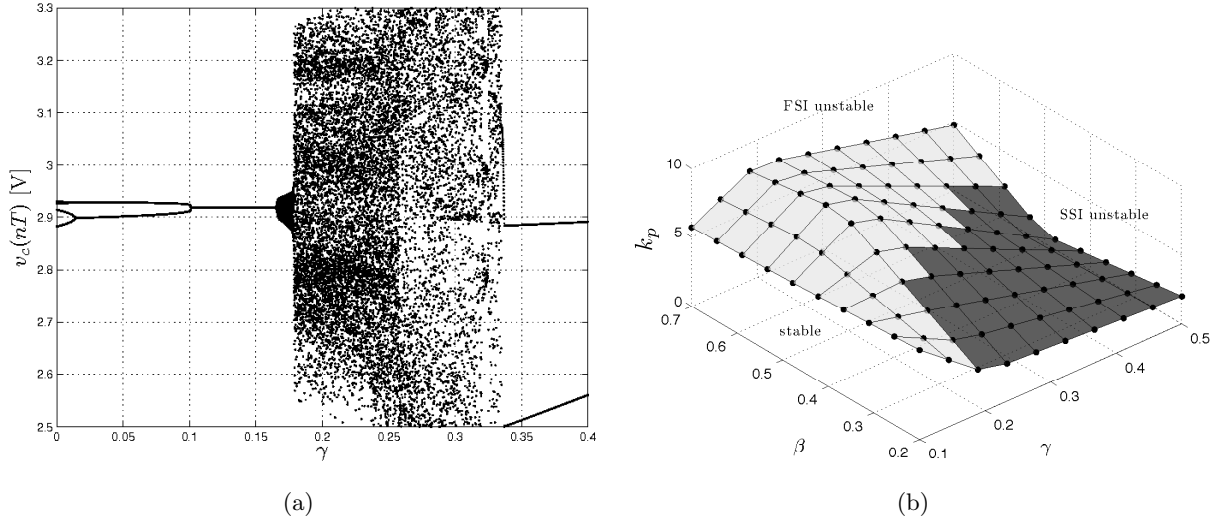


Fig. 7. (a) Bifurcation diagram by sweeping γ in a VMC buck converter with ETDFC for $\beta=0.2$. (b) Stability boundary surface, obtained from numerical simulations, in a VMC buck converter with ETDFC as a function of β and γ . FSI (white) and SSI (black) boundaries are shown.

implementation difficulties in the analog domain. In [Lu *et al.*, 2011] the time-delay magnitude of the TDFC controller has been replaced by a notch and a high-pass filter in order to simplify its implementability but the structure remains similar, hence not being aware to the design-standpoint.

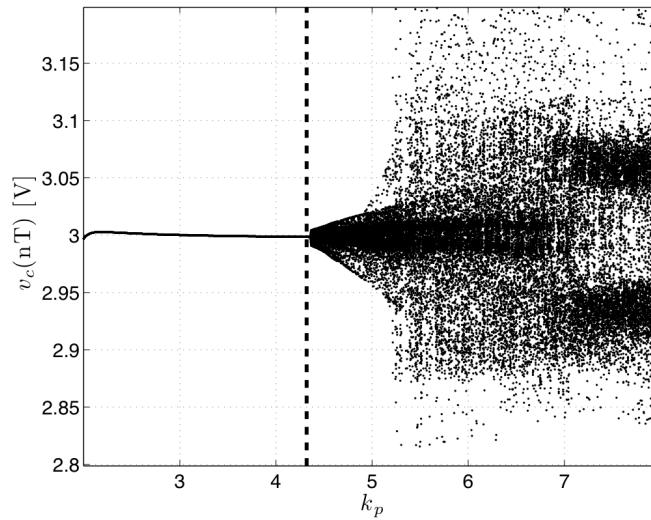


Fig. 8. Bifurcation diagram by sweeping the proportional gain k_p in a VMC buck converter with a pure notch filter ($\xi_1=0$), tuned at half of the switching frequency with $\xi_2=0.001$. Vertical dashed line indicates the stability boundary without controller.

Time-delay-based approaches are based on an additional feedback loop to create a frequency response $G_{FS}(s)$, which provides a comb-like filtering starting with a notch filter at half of the switching frequency. The previous section has shown that their frequency response can be modified by changing γ and β parameters.

This section explores the effect of a stop-band filter in the feedback path whose generic transfer function is:

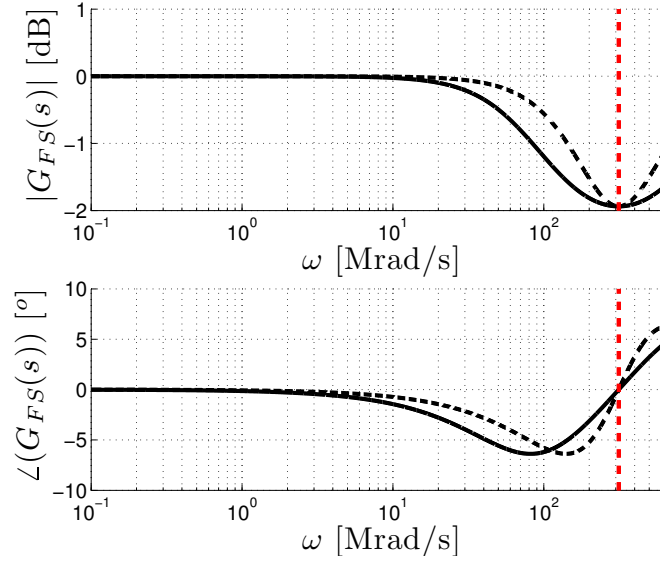


Fig. 9. Bode diagram representation (magnitude and phase) of the stop-band controller as a function of ξ_2 keeping constant the attenuation $\Delta_\xi=0.8$ with $\xi_2=1$ (dash-point) and $\xi_2=2$ (solid). Dashed line indicates half of the switching frequency.

$$G_{FS,notch}(s) = \frac{s^2 + 2\xi_1\omega_n + \omega_n^2}{s^2 + 2\xi_2\omega_n + \omega_n^2} \quad (2)$$

Note that for the case of $\xi_1=0$, the transfer function corresponds to a pure notch filter which only depends upon the parameter ξ_2 , being the notch resonant frequency ω_n to be tuned to one half of the switching frequency i.e: $\omega_n = \omega_s/2$.

The bifurcation diagram in Fig. 8 shows that increasing the proportional gain leads the converter to exhibit SSI, even for low values of ξ_2 ($\xi_2 = 0,001$, high quality factor) because of the phase lag. Note that the bifurcation point $k_p=4.2$ is very close to the one obtained without controller, as it is shown in Fig. 2, but in this case exhibiting SSI instead of FSI.

Alternatively and in a similar way as it has been carried out for ETDFC, it is possible to smooth the magnitude and the phase of the transfer function by moving its zeros in Eq. (2) (for $\xi_1 \neq 0$). The frequency response of the transfer function is shown in Fig. 9, in which the design-space can be described as a function of ξ_2 and the attenuation at half of the switching frequency $\Delta_\xi = \xi_1/\xi_2$ ($\Delta_\xi < 1$).

The exploration of the FSI stability boundary in Fig. 10, obtained from the discrete-time model, unveils similar results as in the ETDFC case. This is, the FSI boundary depends upon the attenuation Δ_ξ and selectivity of the stop-band. The higher the attenuation is, the better stability is obtained in terms of FSI, but, on the other hand, the system is more prone to SSI exhibition. Besides that, by increasing the stop-band width (equivalently to increase ξ_2) the tendency to exhibit SSI is reduced. It is worth mentioning that by increasing ξ_2 , hence increasing the attenuation band, the results are close to those obtained from a buck converter under a simple PI compensator without chaos controller, whose proportional gain before FSI is exhibited, is $k'_{p,crit} = k_{p,crit}/\Delta_\xi$.

4. Repetitive chaos controllers

The previous controllers are based on attenuating the frequency content at half of the switching frequency to extend the stability margin in terms of FSI. However, the use of a so-called repetitive controller, shown in Fig. 11, has been also used for subharmonic control purpose [Escobar *et al.*, 2006; Corradini *et al.*, 2008]. The s -domain representation of such a repetitive controller as a function of parameter γ is:

$$G_{FS}(s) = \frac{e^{sT} + \gamma}{e^{sT} - \gamma} \quad (3)$$

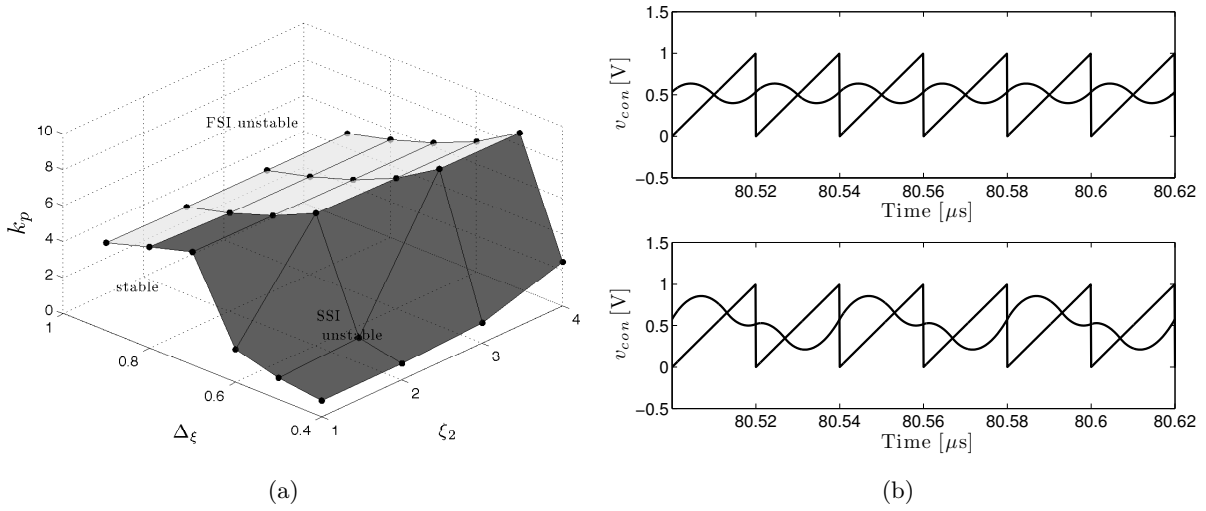


Fig. 10. (a) FSI boundary surface, obtained from a discrete-time model, in a VMC buck converter with a notch controller tuned at half of the switching frequency, as a function of attenuation Δ_ξ and ξ_2 . FSI (white) and SSI (black) boundaries. (b) Time-domain modulator input waveform v_{con} with period-1 behaviour when $k_p=5$ (top figure) and period-2 behaviour when $k_p=6$ (bottom figure). In both cases $\xi_2=2$ and $\Delta_\xi=0.8$.

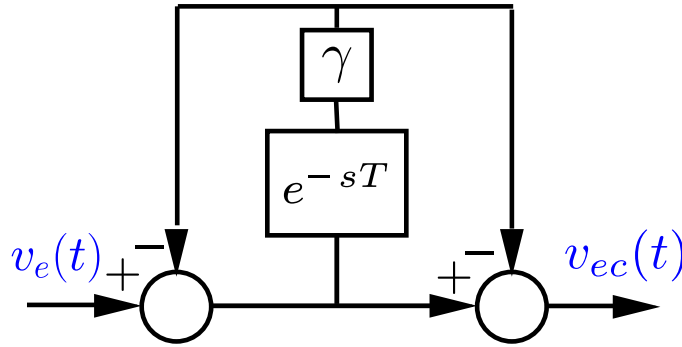


Fig. 11. Feed-forward repetitive controller structure.

The frequency response of this repetitive controller is shown in Fig. 12 along with that of TDFC. Note that comparing with a simple TDFC, apart from attenuating the harmonic at half of the switching frequency, the controller is amplifying not only at the switching frequency harmonics but also at the DC component, hence losing the *non-invasive* nature that previous controllers had.

The bifurcation diagram and the stability boundary in terms of γ and the proportional gain k_p are shown in Fig. 13, which can be compared with the TDFC in Fig. 5, showing that the repetitive controller is less stable in terms of SSI but more stable in terms of FSI. Regarding the SSI observed results, they agree with the frequency domain interpretation, in which more phase lag is added by the controller. However, in terms of FSI, the improvement of the stability margin compared to TDFC can be only attributed to the amplification of switching frequency harmonic.

5. Narrow band amplifier chaos controller

The previous section suggests that FSI control can be accomplished not only by attenuating the harmonic at half of the switching frequency but also amplifying the switching frequency harmonic.

Thus, this section is focused on providing the FSI control functionality from a feasible implementation of such harmonic amplification. This is carried out by using a narrowband amplifier (NBA) centered at the switching frequency. Note that in [Redl & Sun, 2009], enhanced ripple regulators are proposed based on adding a single feedback path with an amplifier that improves the DC regulation while also “amplifies

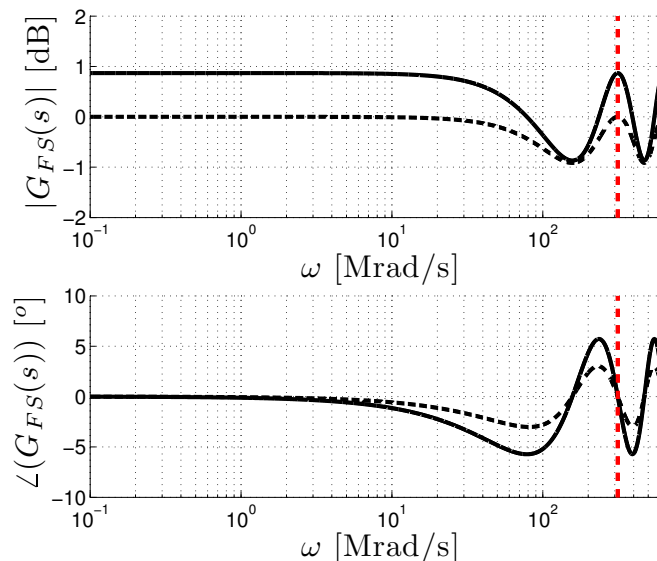


Fig. 12. Bode diagram representation (magnitude and phase) of the repetitive controller with $\gamma=0.05$ (solid) with a repetitive controller (solid) and TDFC (dash). Dashed line indicates the switching frequency

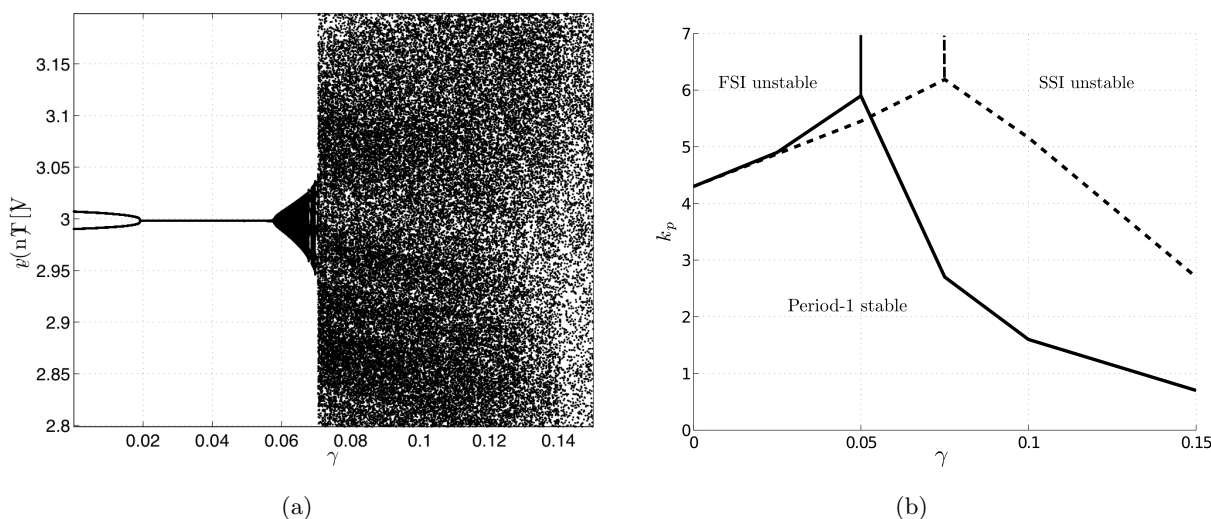


Fig. 13. (a) Bifurcation diagram by sweeping γ (with $k_p=3$) in a VMC buck converter with a repetitive controller and (b) Stability boundary between Period-1, FSI and SSI as a function of γ and k_p with a repetitive controller (solid) and TDFC (dashed line).

and shapes" the ripple voltage. The work points out that by means of such amplifier, based on a PID, the controller can improve the FSI. However, in that work it is not justified why FSI is eliminated and a clear cause of the effect of such amplifier upon the FSI has not been provided. Also, the approach is not applied for the PWM VMC control but for ripple controllers.

The transfer function of the FSI chaos controller NBA $G_{FS}(s)$ can be described as in the case of a notch filter in Eq. (2) but with $\Delta_\xi > 1$ and the center frequency tuned to the switching frequency, $\omega_n = 2\pi f_s$. The magnitude and phase of such transfer function in the frequency domain is shown in Fig. 14. Apart from the amplification at the switching frequency harmonic, a key additional advantage is the fact that it notably improves the SSI boundary by adding a phase lead before the switching frequency (note that no additional phase is added at the switching frequency).

Its effect upon FSI boundary is depicted in Fig. 15, which shows the stability boundary surface as a

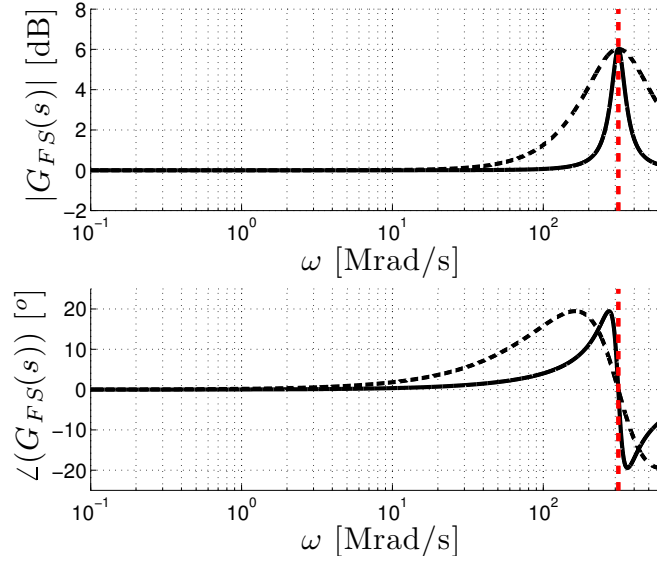


Fig. 14. Bode diagram representation (magnitude and phase) of an NBA tuned to the switching frequency (vertical dashed-line) with $\Delta_\xi=2$ and $\xi_2=0.1$ (solid) and $\xi_2=0.5$ (dash).

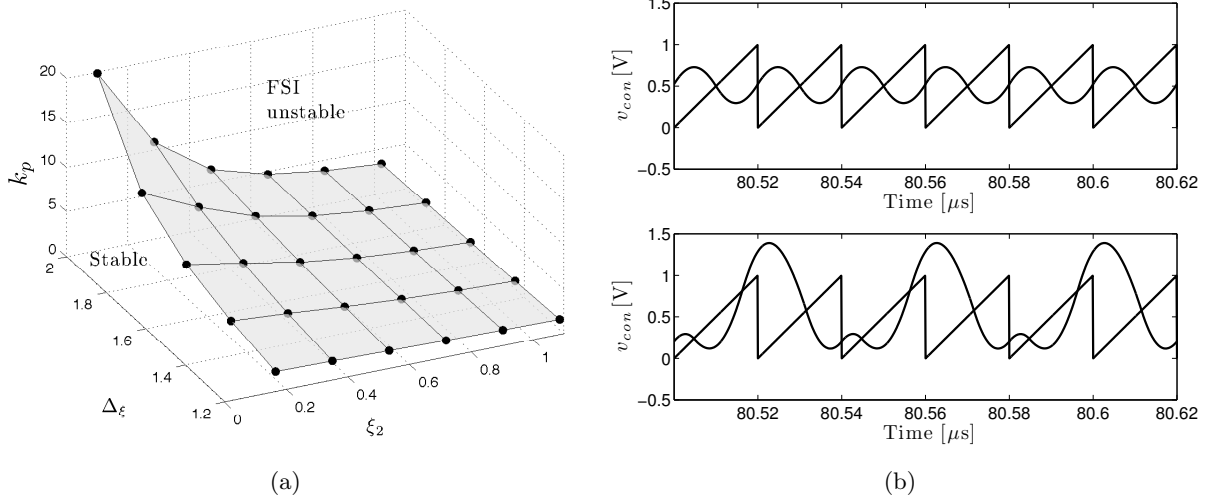


Fig. 15. (a) Stability surface obtained from the discrete-time model as a function of the proportional gain k_p and parameters ξ_2 and Δ_ξ . (b) Time-domain modulator input waveform v_{con} with period-1 behaviour when $k_p=5$ (top figure) and period-2 behaviour when $k_p=8$ (bottom figure). In both cases $\xi_2=0.6$ and $\Delta_\xi=1.5$.

function of Δ_ξ and ξ_2 . On the one hand, the parameter ξ_2 , which has a direct effect upon the width of the amplification band, has an important effect upon the stability boundary so that as it increases, the FSI boundary is worsened. This suggests that the benefits of the NBA controller on stability are limited by such bandwidth, namely when both harmonics at the switching frequency and its half are amplified the FSI boundary is not modified. On the other hand, it is possible to observe that the higher the amplification is, the more stable the system is in terms of FSI.

The discussion and characterization of chaos controllers have been hitherto limited to the proportional gain k_p since it is one of the parameters that affects the high-frequency transfer function magnitude, and then ripple component of the control path, but without modifying the phase. As it was mentioned at the beginning of this work, the indirect aim of a chaos controller, apart from obviously improving the stability margin, is that such improvement allows to expand the design-space towards miniaturization (for instance

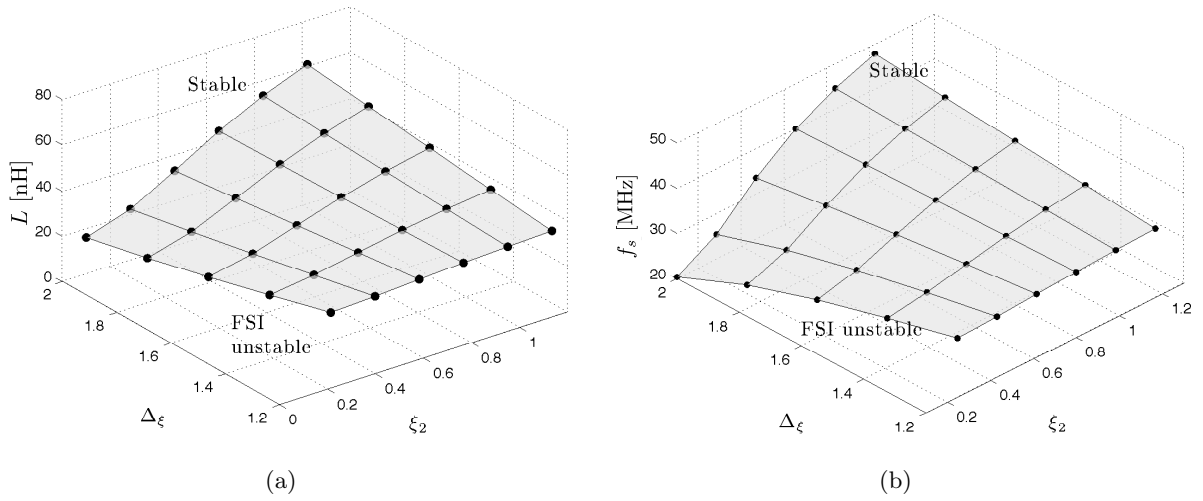


Fig. 16. FSI boundary, obtained from the discrete-time model, of a VMC buck converter with an NBA as a function of parameters Δ_ξ , ξ_2 and (a) the inductance L and (b) the switching frequency f_s .

reducing the inductance value, which is related to the system area), without losing stability.

Simulations in Fig. 16 show the stability boundary as a function of the inductance (related to area/volume occupancy) and switching frequency (related to efficiency). Note that both surfaces are similar and the stability boundary is clearly improved, allowing to reduce both parameter values without losing stability, when $\xi_2 < 1$ and $\Delta_\xi > 1$ (a narrow band amplification) with regards to the case of not using such controller ($\Delta_\xi = 1$).

6. Stability margins of the different controllers: a benchmark comparison

Up to now, different FSI controller approaches have been explored individually in terms of stability and hence this section is focused on comparing them in stability terms. The parameters used in this section are the same as in the previous sections but with $V_{ref} = 1.2$ V.

The stability boundaries, obtained by numerical simulations along with the discrete-time model, of TDFC, ETDFC, notch-based controller, NBA are shown in Fig. 17. These boundaries have been obtained by sweeping the PI compensator parameters, namely the proportional gain k_p and the zero ω_{z1} , due to their capability to explore a wide design-space range including both FSI and SSI boundaries.

It is possible to observe that FSI appears when the proportional gain is increased and ω_{z1} lower ω_{RC} (depending upon the control), whereas SSI appear as ω_{z1} is closer to ω_{RC} .

The exploration shows that time-delay-based controllers have limited benefits, because of their negative effect upon SSI boundary, hence reducing their advantages in terms of overall stability. It is interesting to observe that the notch-based approach, which has been derived from such time-delay-based controllers, by properly adjusting the damping factors (ξ_1 and ξ_2), can result in improved behavior.

The alternative approaches based on amplifying the switching frequency harmonic show a better behavior in terms of overall stability. The simple NBA is the only controller that concurrently improves both stability boundaries.

7. Conclusions

This paper has revisited the controllers for fast-scale instability from a frequency domain standpoint in order to better understand their principle of operation, study their effect upon stability boundaries and provide new approaches to control such instabilities that facilitates the implementability of the controllers and the performance of the system.

First the paper unveils that previous time-delay controllers are based on a comb-filter attenuating

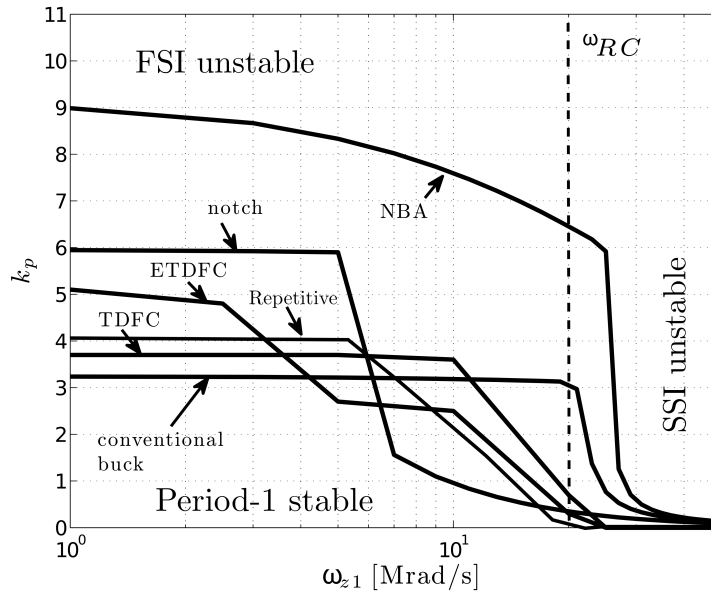


Fig. 17. Stability boundaries, obtained from the respective discrete-time model and numerical simulations, of a VMC buck converter as a function of the PI compensator parameters k_p and ω_{z1} by using different FSI controllers, adding a TDFC with $\gamma=0.05$; a ETDFC with $\gamma = 0.2$ and $\beta=0.5$; a notch-based controller with $\xi_1=1.2$ and $\xi_2 = 2$; a repetitive controller with $\gamma=0.05$; an NBA with $\xi_1 = 0.1$ and $\xi_2 = 0.4$. $V_{ref}=1.2$ V

multiples of one half the switching frequency and demonstrates that their benefits in terms of fast-scale stability boundary is detrimental to slow-scale boundary, hence limiting their global stability boundary. Furthermore, the work has proposed a single notch-based controller as a substitute of such comb-filters avoiding the implementation of time-delay modules, and obtaining similar results in terms of stability.

The study has also proposed an alternative fast-scale instability control method based on amplifying the harmonic at the switching frequency, demonstrating its benefits on both fast-scale and slow scale stability boundary. The work demonstrates that this controller allows to extend the fast-scale stability boundary by exploring different parameters representative of converter miniaturization trends, and that such boundaries depend upon the amplification band, provided that this is narrow enough to attenuate the harmonic at the half of the switching frequency, and the amplification factor.

Finally, the overall stability analysis is studied by benchmarking and comparing all the previous controllers showing that only in the case of a narrow band amplifier, the control of fast-scale instability is not detrimental of slow-scale dynamic behavior, hence it can be considered as a key enabling controller to improve converter miniaturization without losing stability.

References

- Allard, B., Trochut, S., Lin-Shi, X. & Retif, J.-M. [2004] "Control design for integrated switch-mode power supplies: a new challenge?" *IEEE Power Electronics Specialists Conference (PESC'04)*, pp. 4492–4497, doi:10.1109/PESC.2004.1354794.
- Angulo, F., Burgos, J. & Olivar, G. [2007] "Chaos stabilization with TDAS and FPIC in a buck converter controlled by lateral PWM and ZAD," *Mediterranean Conference on Control Automation MED '07*, pp. 1–6, doi:10.1109/MED.2007.4433846.
- Batlle, C., Fossas, E. & Olivar, G. [1997] "Stabilization of periodic orbits of the buck converter by time-delayed feedback," *International Journal of Circuit Theory and Applications* **27**, 617–631.
- Chen, G. & Dong, X. [1993] "Control of chaos-a survey," *IEEE Conference on Decision and Control*, pp. 469–474, doi:10.1109/CDC.1993.325103.
- Chen, Y., Tse, C. K., Qiu, S.-S., Lindenmuller, L. & Schwarz, W. [2008] "Coexisting fast-scale and slow-

- scale instability in current-mode controlled DC/DC converters: Analysis, simulation and experimental results,” *IEEE Transactions on Circuits and Systems I: Regular Papers* **55**, 3335–3348, doi:10.1109/TCSI.2008.923282.
- Corradini, L., Mattavelli, P., Tedeschi, E. & Trevisan, D. [2008] “High-bandwidth multisampled digitally controlled DCDC converters using ripple compensation,” *IEEE Transactions on Industrial Electronics* **55**, 1501–1508, doi:10.1109/TIE.2008.917144.
- di Bernardo, M., Garefalo, F., Glielmo, L. & Vasca, F. [1998] “Switchings, bifurcations, and chaos in DC/DC converters,” *IEEE Transactions on Circuits and Systems I: Fundamental Theory and Applications* **45**, 133–141.
- Escobar, G., Martinez, P., Leyva-Ramos, J. & Mattavelli, P. [2006] “A negative feedback repetitive control scheme for harmonic compensation,” *IEEE Transactions on Industrial Electronics* **53**, 1383–1386, doi:10.1109/TIE.2006.878293.
- Fossas, E. & Olivar, G. [1996] “Study of chaos in the buck converter,” *IEEE Transactions on Circuits and Systems I: Fundamental Theory and Applications* **43**, 13–25, doi:10.1109/81.481457.
- Hamill, D. C. & Jeffries, D. J. [1988] “Subharmonics and chaos in a controlled switched-mode power converter,” *IEEE Transactions on Circuits and Systems I* **35**, 1059–1061.
- Krein, P. & Bass, R. [1990] “Types of instability encountered in simple power electronic circuits: unboundedness, chattering, and chaos,” *Applied Power Electronics Conference and Exposition (APEC’90)*, pp. 191–194.
- Lu, W. G., Zhou, L. W., Luo, Q. M. & Wu, J. K. [2011] “Non-invasive chaos control of DC-DC converter and its optimization,” *International Journal of Circuit Theory and Applications* **39**, 159–174.
- Mazumder, S. K., Nayfeh, A. H. & Boroyevich, D. [2001] “Theoretical and experimental investigation of the fast- and slow-scale instabilities of a DC-DC converter,” *IEEE Transactions on Power Electronics* **16**, 201–216, doi:10.1109/63.911144.
- Middlebrook, R. & Cuk, S. [1976] “A general unified approach to modelling switching-converter power stages,” *Power Electronics Specialists Conference (PESC’76)*, pp. 18–34.
- Poddar, G., Chakrabarty, K. & Banerjee, S. [1998] “Control of chaos in DC-DC converters,” *IEEE Transactions on Circuits and Systems I: Fundamental Theory and Applications* **45**, 672–676, doi:10.1109/81.678489.
- Pyragas, K. [1992] “Continuous control of chaos by self-controlling feedback,” *Physics Letters A* **170**, 421–428, doi:10.1016/0375-9601(92)90745-8.
- Pyragas, K. [1995] “Control of chaos via extended delay feedback,” *Physics Letters A* **206**, 323–330, doi:DOI:10.1016/0375-9601(95)00654-L.
- Redl, R. & Sun, J. [2009] “Ripple-based control of switching regulators: An overview,” *IEEE Transactions on Power Electronics* **24**, 2669–2680, doi:10.1109/TPEL.2009.2032657.
- Rodriguez, E., Guinjoan, F., El Aroudi, A. & Alarcon, E. [2012] “A ripple-based design-oriented approach for predicting fast-scale instability in *dc-dc* switching power supplies,” *IEEE Transactions on Circuits and Systems I: Regular paper* **59**, 215–227, doi:10.1109/TCSI.2011.2161396.
- Tse, C. K. [1994] “Chaos from a buck switching regulator operating in discontinuous mode,” *Int. J. Circuit Theory Applicat.* **22**, 263–278.
- Xiong, X. , Tse, C.K. and Ruan, X. [2013] “Smooth and Non-Smooth Bifurcations in Multi-Structure Multi-Operating-Mode Hybrid Power Systems”, *Int. J. Bifurcations & Chaos*, **23**, no. 5, pp. 1350094, May 2013.
- Zhao, Y., Feng, J. & Chen, Y. [2013] “Bifurcation Investigation and Stability Analysis for Peak Current Mode Input-Series Output-Parallel DC-DC Converters,” *Int. J. Bifurcations & Chaos* **23**, no. 07, 13 pages, 2013.